

Article

Selective and Effective Gold Recovery from Printed Circuit Boards and Gold Slag Using Amino-Acid-Functionalized Cellulose Microspheres

Fulai Hao ^{1,2}, Jifu Du ^{3,*} , Lifang Peng ⁴, Manman Zhang ⁴, Zhen Dong ⁴, Yanbai Shen ^{1,*}  and Long Zhao ^{4,*}¹ School of Resources and Civil Engineering, Northeastern University, Shenyang 110819, China² Changchun Gold Research Institute, China National Gold Group Co., Ltd., Changchun 130012, China³ School of Nuclear Technology and Chemistry & Biology, Hubei University of Science and Technology, Xianning 437100, China⁴ State Key Laboratory of Advanced Electromagnetic Engineering and Technology, School of Electrical and Electronic Engineering, Huazhong University of Science and Technology, Wuhan 430074, China

* Correspondence: duzidedu@163.com (J.D.); shenyanbai@mail.neu.edu.cn (Y.S.); zhaolong@hust.edu.cn (L.Z.)

Abstract: The hydrometallurgical recovery of gold from electronic waste and gold slag is a hot research topic. To develop a cost-effective and environmentally friendly adsorbent for gold recovery, four types of amino-acid (arginine, histidine, methionine, and cysteine)-functionalized cellulose microspheres were prepared via a radiation technique. The adsorption performance of the amino acid resins toward Au(III) ions was systematically investigated by batch experiments. The amino acid resins could absorb Au(III) ions at a wide pH range. The adsorption process was followed by the pseudo-second-order model and Langmuir model. The theoretical maximum adsorption capacity was calculated as 396.83 mg/g, 769.23 mg/g, 549.45 mg/g, and 636.94 mg/g for ArgR, HisR, MetR, and CysR, respectively. The amino acid resins could effectively and selectively recover trace Au(III) ions from the leaching solutions of printed circuit board and gold slag waste. Lastly, the mechanism underlying amino acid resin's Au(III) ion recovery capability was investigated by FTIR, XRD, and XPS analyses. This work describes a series of cost-effective gold adsorbents with excellent selectivity and adsorption capacity to boost their practical application.

Keywords: amino acid; cellulose microspheres; Au recovery; selectivity



Citation: Hao, F.; Du, J.; Peng, L.; Zhang, M.; Dong, Z.; Shen, Y.; Zhao, L. Selective and Effective Gold Recovery from Printed Circuit Boards and Gold Slag Using

Amino-Acid-Functionalized Cellulose Microspheres. *Polymers* **2023**, *15*, 321. <https://doi.org/10.3390/polym15020321>

Academic Editor: Serena Coiai

Received: 11 November 2022

Revised: 31 December 2022

Accepted: 2 January 2023

Published: 8 January 2023



Copyright: © 2023 by the authors. Licensee MDPI, Basel, Switzerland. This article is an open access article distributed under the terms and conditions of the Creative Commons Attribution (CC BY) license (<https://creativecommons.org/licenses/by/4.0/>).

1. Introduction

As a popular precious metal, gold (Au) is widely used in the medical, electronic, and electrical industries due to its special properties, such as excellent electrical conductivity and outstanding corrosion resistance [1]. The contradiction between the growing demand for resources in the Earth's crust and their limited nature has gradually increased the price of Au. Thus, Au recovery from products utilizing these materials, especially electronic waste and gold slag, has received more and more attention [2]. An appropriate recycling approach can not only retrieve the gold from the e-waste, but also reduce the environmental toxicity of e-waste [3].

There are several technologies for Au recovery using leaching solutions, such as cementation, chemical precipitation, solvent extraction, biosorption, electrolysis, membrane separation, ion exchange, and adsorption [1,4,5]. Among these techniques, adsorption has been considered a promising technology to recover trace precious metals from wastewater due to its low cost, great reusability, and easy operation [6,7].

By now, various adsorbents, such as active carbon [8], multiwalled carbon nanotubes [9], covalent organic frameworks [10], metal-organic frameworks [11], nanoparticles [12,13], melanin-based polymers such polydopamine [14,15], natural polymers (cellulose [16,17], and chitosan [18,19]), among others, have been used for waste remediation. Among them, microcrystalline cellulose (MCC) has many advantages, such as

sustainability, hydrophilicity, biodegradability, and easy functionalization, which make it very suitable as an adsorbent substrate [17,20–22]. Although MCC has many hydroxyl groups in its chemical structure, the adsorption performance of pure MCC is not satisfactory. So, it is necessary to improve the adsorption property via functionalization. The functional groups for Au(III) ion adsorption are often composed of sulfur and nitrogen atoms such as amine [10], thiourea [20], thiol [23], etc. Dong et al. observed that the maximal adsorption quantities of three novel *n*-aminomethylpyridine (*n*-AMP, *n* = 2, 3, 4)-modified cellulose compounds for Au(III) ions were 1.548, 1.915, and 2.418 mmol/g, respectively [24]. Norasikin and colleagues functionalized lignocellulosic coconut pith (LCP) with 3-aminopropyltriethoxysilane (APS) as a Au(III) ion adsorbent (APS-LCP), which expressed a great adsorption capacity of 261.36 mg/g at 30 °C [25].

In recent years, amino-acid-functionalized materials have attracted much attention because amino acid contains carboxylic acid, amine, and sulfhydryl groups (–COOH, –NH₂, and –SH), which can be easily conjugated to metal ions. Several researchers reported the adsorption and reduction of Au(III) ions by amino acid [11,26,27]. However, very little investigation has been reported for Au recovery from a practical leaching solution of printed circuit boards (PCBs) and gold slag using amino-acid-functionalized materials.

Radiation-induced grafting polymerization (RIGP) is a powerful technique used to modify polymers because RIGP can generate free radicals and form grafting, which is relevant for subsequent chemical modification. This method can reach a high grafting yield (GY) quickly without heating [21,24]. Then, high functional group density can be obtained through subsequent chemical modification such as the ring-opening reaction.

In this study, four types of amino-acid (arginine, histidine, methionine, and cysteine)-functionalized cellulose compounds were prepared via radiation for Au recovery. The Au(III) ion adsorption performance of amino acid resin using the simulated and practical leaching solutions was systematically investigated.

2. Materials and Methods

2.1. Materials

The MCC microsphere was supplied by Asahi Kasei Chemicals Corporation (Tokyo, Japan). Chloroauric acid (HAuCl₄·4H₂O), glycidyl methacrylate (GMA), and Tween 20 were supplied by Sinopharm Chemical Reagent Co., Ltd. Arginine, histidine, methionine, and cysteine were purchased from Mecklin Chemical Reagent Co., Ltd.

2.2. Preparation of Amino Acid Resins

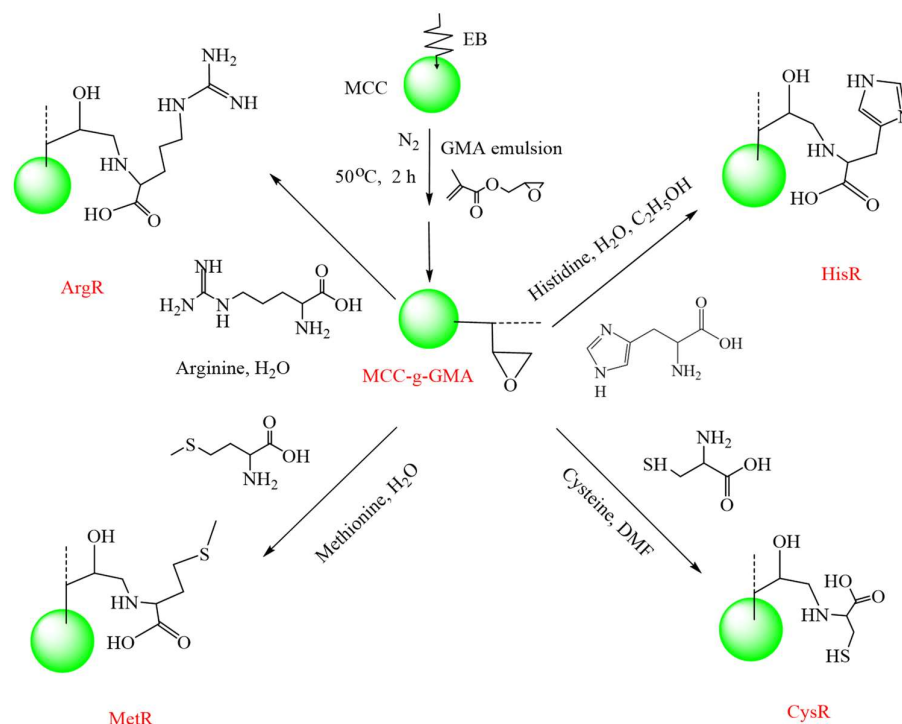
The amino-acid-functionalized cellulose was prepared through two steps. Firstly, GMA was grafted on the MCC microsphere using the pre-irradiation grafting technique as reported in previous works [28–30]. First, the MCC microsphere (5.0 g) was vacuum-sealed in PE bags. The samples were irradiated with an absorbed dose of 10 kGy with an EB accelerator under the cooling action of dry ice. The irradiated bag was injected with 50 mL of deoxygenated GMA emulsion solution (30 wt% GMA and 3 wt% Tween 20) and put into a water bath at 50 °C for 2 h. Subsequently, the GMA-grafted microsphere (MCC-g-GMA) was separated and washed with de-ionized water, and then dried to a constant weight. The mass gain was calculated using Equation (1):

$$\text{Mass gain} = \frac{m_g - m_0}{m_0} \times 100\% \quad (1)$$

where m_0 and m_g are the weight of MCC and MCC-g-GMA, respectively.

Secondly, the MCC-g-GMA (2.0 g) was immersed into different solutions and allowed to react at 80 °C for 24 h. The solution was divided into four types: 20 mL of 10 wt% arginine aqueous solution, 20 mL of 20 wt% cysteine DMF solution, 20 mL of 10 wt% methionine aqueous solution, and 20 mL of 10 wt% histidine 50%H₂O/50% EtOH solution. After the reaction, these final products were washed with de-ionized water and dried at

60 °C to a constant weight. Scheme 1 shows the preparation procedure for the amino acid resins.



Scheme 1. The preparation procedure for the amino acid resins.

The molar amount of amino acid (MAAA) on the unit amino acid resins was calculated by Equation (2):

$$\text{MAAA} = \frac{m_r - m_g}{m_r \times \text{Mw}_{\text{AA}}} \quad (2)$$

where m_g and m_r are the mass of the MCC-g-GMA and amino acid resins. Mw_{AA} is the molecular weight of a different amino acid.

2.3. Characterization

Fourier transform infrared spectroscopy (FTIR) spectra were recorded on an FTIR spectrophotometer (Bruker Tensor 207) in the wavenumber range of 4000–400 cm^{-1} . The surface morphology was studied with a scanning electron microscope (SEM, Hitachi SU8000, Japan). The weightlessness curve was recorded on a thermogravimetric analyzer (TGA, TGA 55, TA Instrument mode 600) at temperatures ranging from room temperature to 800 °C at a heating rate of 10 °C/min in a nitrogen atmosphere. An X-ray diffractometer (XRD, Rigaku Corporation, Japan) was applied to capture the pattern images of the materials. The specific surface area of the amino acid resins was measured using the Brunauer–Emmett–Teller method (BET, ASAP2420-4MP Micromeritics, Norcross, GA, USA). The X-ray photoelectron spectroscopy (XPS) spectra were recorded using an AXIS-Ultra DLD instrument from Kratos Analytical (Shimadzu, Kyoto, Japan) with a monochromator using Al-K α radiation.

2.4. Adsorption Experiments

A total of 0.01 g of adsorbent was dispersed in 10 mL of Au(III) ion solution. At 30 °C, the glass bottle was shaken in a beaker at 160 rpm. The pH effect was conducted with pH 1–6 and contact time 24 h. The adsorption kinetics were explored at different contact times, from 0.25 to 36 h, at pH 2. The adsorption isotherms were conducted with the initial concentration of 50 to 1000 mg/L and contact time of 24 h. The NaCl effect was investigated at a contact time of 24 h and initial Au(III) ion concentration of 0.1 mmol/L at pH 2. The reuse property was probed at a contact time of 24 h and initial concentration of 100 mg/L

at pH 2. The concentration of metal ions was analyzed using the ICP-OES (Agilent 5110, Palo Alto, CA, USA).

The number of Au(III) ions adsorbed by amino acid resins at a certain time (Q_t) was calculated using Equation (3):

$$Q_t = \frac{(C_0 - C_t) \times V}{m} \quad (3)$$

where C_0 and C_t are the concentration of Au(III) ions before and after adsorption, respectively; Q_e represents the adsorption capacity when the adsorption reached equilibrium. V and m are the volume of the solution and the weight of the amino acid resins.

3. Results and Discussion

3.1. Preparation and Characterization

MCC-g-GMA with a mass gain of 230% was used as the substrate for amino acid modification. Different amino acid resins were obtained after the ring-opening reaction between the epoxy group of GMA and the amine group of amino acid. For the reaction in 20 mL of arginine aqueous solution, 20 mL of cysteine DMF solution, 20 mL of methionine aqueous solution, and 20 mL of histidine 50% H_2O /50% EtOH solution, the same mass gain, approximately 20%, was obtained.

Considering the molecular weight (174.20, 155, 149.21, and 121.16 for arginine, histidine, methionine, and cysteine), the MAAA of ArgR, HisR, MetR, and CysR was 1.1263, 1.1203, 1.2408, and 1.5011 mmol/g).

FTIR spectra of MCC, MCC-g-GMA, and the amino acid resins are demonstrated in Figure 1. For MCC-g-GMA, there were new peaks at 905 and 847 cm^{-1} , which are the characteristic peaks of epoxy groups [24]. This indicates that GMA was successfully grafted onto MCC. The new characteristic peaks at 1577, 1163, and 1058 cm^{-1} were seen in the spectrum of ArgR, which was related to the vibration of N-H and C-N of arginine [28,31]. In the spectrum of HisR, the vibration adsorption of the N-H (1599 cm^{-1}) and C-N (1161 and 1061 cm^{-1}) bond were observed. There were two weak peaks at 748 and 669 cm^{-1} in the MetR spectrum, which are characteristic peaks of the C-S bond [32]. In addition, the new peaks at 1161 and 1066 cm^{-1} are characteristic peaks of the C-N bond. For CysR, the characteristic peaks of C-S and C-N bonds at 750, 619 cm^{-1} , 1163, and 1059 cm^{-1} were observed. Additionally, the intensity of the characteristic peaks of the epoxide group significantly decreased after amino acid functionalization. So, the synthesis of the amino acid resins was obviously successful.

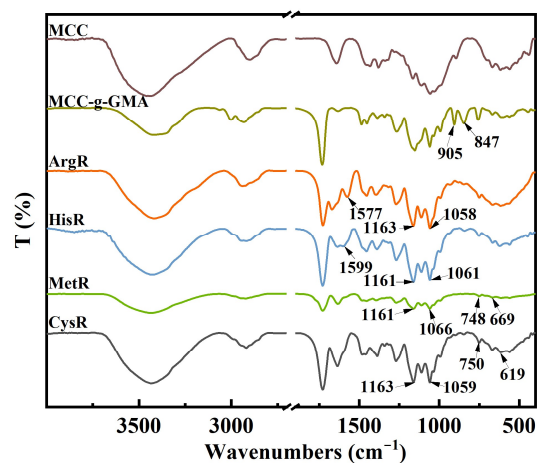


Figure 1. FTIR image of MCC, MCC-g-GMA, and the amino acid resins.

Figure S1 shows the SEM images of MCC, MCC-g-GMA, and the amino acid resins. It can be seen that the diameter of the modified materials increased, which proves the successful introduction of GMA and amino acids to a certain extent. In addition, Table S1

shows the BET surface areas of materials before and after modification. The BET surface area values of the amino acid resins were too low to prove their porous structures.

3.2. Batch Adsorption

3.2.1. Effect of pH

The solution pH plays a vital role in the adsorption of metal ions. The influence of pH on the adsorption capacity (Q_e) of amino acid adsorbents at the initial concentrations of 100 and 400 mg/L is shown in Figure 2. At the lower initial concentration of 100 mg/L, the Au (III) ion adsorption capacity of amino acid adsorbents had almost no effect at pH 1–6. The Au(III) ion adsorption capacity at the higher initial concentration of 400 mg/L firstly increased with the increasing pH and then reached a maximum at about pH 2. Under acidic conditions, N atoms on the amino acid adsorbents were protonated to form positive charge centers, which easily attracted AuCl_4^- . At pH 1, the concentration of HCl increased, and the increase in the ionic strength and shield effect reduced the number of Au(III) ions adsorbed. With the further increase in pH ($\text{pH} > 5$), the concentration of OH^- in the solution increased, and the adsorption competition between OH^- and AuCl_4^- also reduced the number of Au(III) ions absorbed. Meanwhile, the Au(III) ion adsorption capacity of non-functionalized MCC and MCC-g-GMA at pH 1–6 is demonstrated in Figure S2, being less than 15 mg/g. This indicates that amino acid functionalization greatly improved the Au(III) ion adsorption capacity.

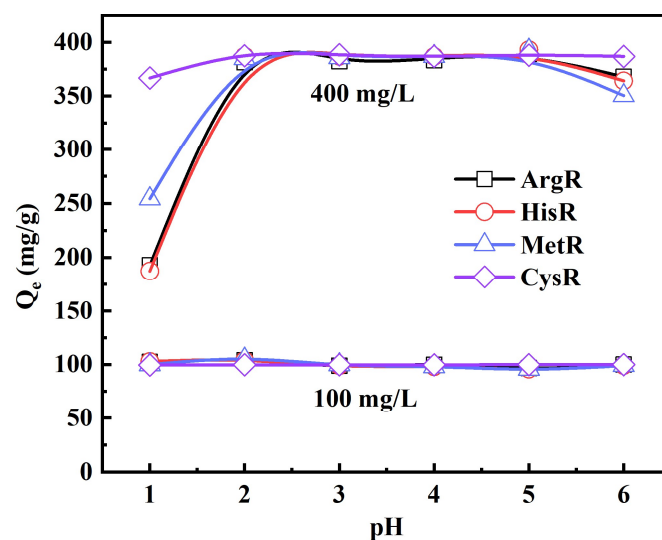


Figure 2. Effect of pH on Au (III) adsorption by amino acid resins ($C_0 = 100$ and 400 mg/L, adsorbent mass = 10 mg, volume = 10 mL, $T = 30$ °C, contact time = 24 h).

3.2.2. Adsorption Kinetics: Effect of Adsorption Time

In order to explore the adsorption kinetics, the effect of adsorption time on adsorption capacity was investigated and is shown in Figure 3 ($C_0 = 100$ mg/L) and Figure S3 ($C_0 = 400$ mg/L). It can be seen that the adsorption capacity increased rapidly initially because there were many active sites on the surface of the adsorbents. With the increase in contact time, the active sites of the adsorbents were occupied continuously, and the adsorption gradually reached equilibrium. The experimental data were fitted by pseudo-first-order (Equation (4)) and pseudo-second-order models (Equation (5)) to evaluate the adsorption kinetics. The initial adsorption rate h_0 (mg/g·min) ($t \rightarrow 0$) is described by Equation (6) [33,34].

$$Q_t = Q_e \left(1 - e^{-k_1 t}\right) \quad (4)$$

$$Q_t = \frac{k_2 Q_e^2 t}{1 + k_2 Q_e t} \quad (5)$$

$$h_0 = k_2 Q_e^2 \tag{6}$$

where Q_e and Q_t (mg/g) are the adsorption mass of Au(III) ions at equilibrium or any time t .

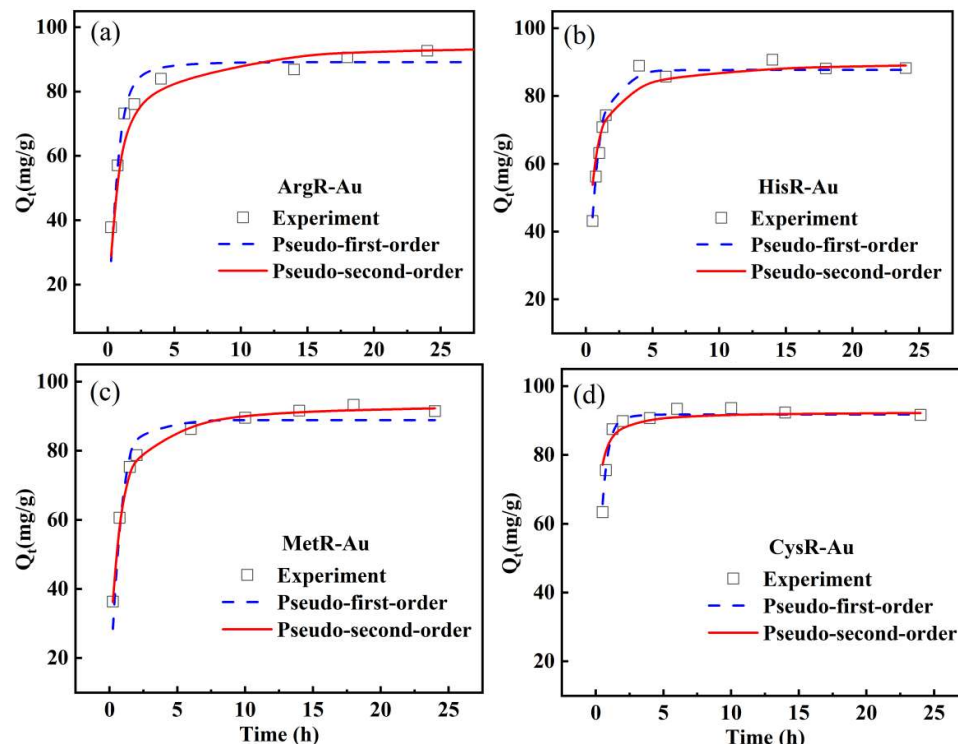


Figure 3. The adsorption kinetics of ArgR (a), HisR (b), MetR (c) and CysR (d) for Au(III) ions ($C_0 = 100$ mg/L, adsorbent mass = 10 mg, volume = 10 mL, pH = 2, $T = 30$ °C).

The kinetic parameters obtained by fitting are listed in Table 1 ($C_0 = 100$ mg/L) and Table S2 ($C_0 = 400$ mg/L). The results show that the adsorption of Au (III) by the amino acid resins accorded with the pseudo-second-order kinetic model, suggesting the mechanism by which Au(III) ions were absorbed was chemical adsorption [35,36].

Table 1. Kinetic parameters obtained from kinetic models.

Adsorbents	Pseudo-First-Order Model			Pseudo-Second-Order Model			
	k_1 (h^{-1})	Q_e (mg/g)	R^2	k_2 (g/(mg·h))	Q_e (mg/g)	R^2	h_0
ArgR	1.4596	89.1507	0.9098	0.0182	95.0570	0.9995	164.45
HisR	1.5424	88.8839	0.9427	0.0268	93.8086	0.9997	235.84
MetR	1.4036	87.6844	0.9533	0.0327	90.2527	0.9995	266.36
CysR	2.5200	91.7400	0.9809	0.1080	92.5926	0.9998	925.96

3.2.3. Adsorption Isotherms: Effect of Initial Concentration

In order to explore the maximum adsorption capacity of different amino acid resins for Au(III), the adsorption capacity of each amino acid resin under different initial concentrations of Au(III) was studied. As shown in Figure 4, the amount of Au (III) adsorbed on the adsorbents sharply increased with the increase in Au (III) concentration, and then tended to approach a constant value at a higher concentration. The Langmuir (Equation (7)) and Freundlich (Equation (8)) models were used to fit the experimental data [37,38].

$$Q_e = \frac{Q_m k_L C_e}{1 + (k_L C_e)} \tag{7}$$

$$Q_e = k_F C_e^{1/n} \tag{8}$$

where Q_e (mg/g) and C_e (mg/L) are the equilibrium adsorption capacity and equilibrium concentration, and Q_m (mg/g) is the maximum adsorption capacity.

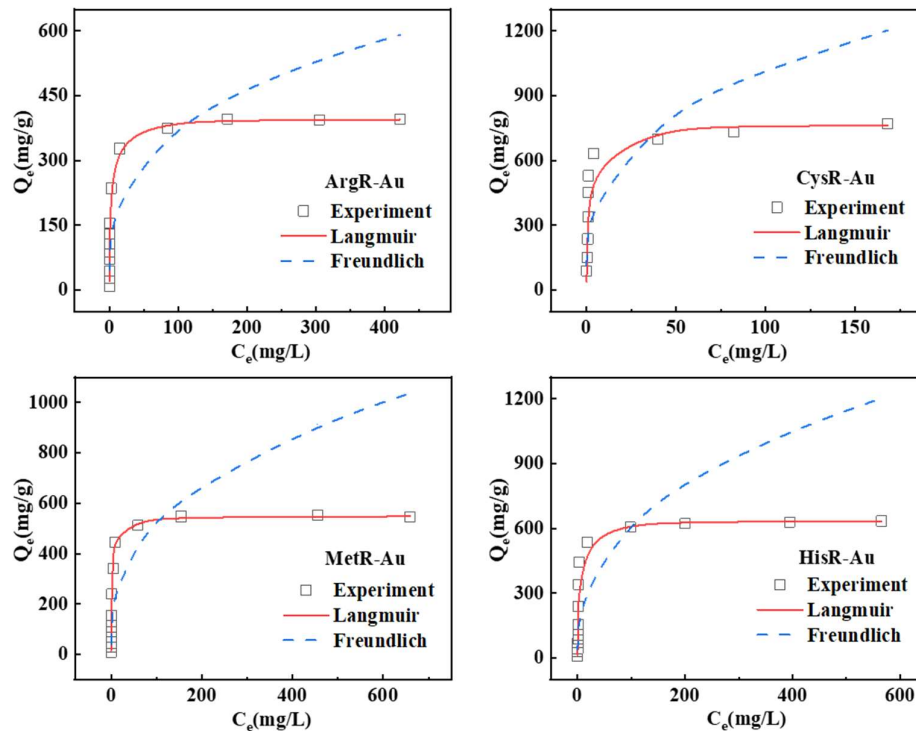


Figure 4. The adsorption isotherms for Au (III) by amino acid resins (adsorbent mass = 10 mg, volume = 10 mL, pH = 2, T = 30 °C, contact time = 24 h).

The adsorption and fitting results are summarized in Table 2. The higher fitting coefficients of the Langmuir model for amino acid resins were greater than 0.99, indicating that the adsorption isotherms of the amino acid resins for Au(III) are more accordance with the Langmuir adsorption isotherm model, and Au(III) ions were absorbed by a monolayer distribution [39]. Theoretically, the maximum Au (III) adsorption capacity of the four amino acid resins is 396.83 mg/g, 769.23 mg/g, 549.45 mg/g, and 636.94 mg/g, suggesting that all amino acid resins are good Au-adsorbing materials.

Table 2. Adsorption isotherm parameters for Au(III) absorbed by amino acid resins.

Adsorbents	Langmuir			Freundlich		
	Q_m (mg/g)	K_L (L/mg)	R^2	K_F (mg/g)	n	R^2
ArgR	396.8	0.4903	0.9999	92.1751	3.2527	0.6644
HisR	636.9	0.3668	0.9999	114.5304	2.6953	0.7217
MetR	549.5	0.5741	0.9999	112.2277	2.9200	0.7470
CysR	769.2	0.7927	0.9993	262.4000	3.3653	0.7364

Q_m is an important parameter for assessing adsorption performance. Table 3 compares the Au(III) adsorption capacity of the amino acid adsorbents and other adsorbents. As can be seen, the amino acid adsorbents exhibited an excellent adsorption capacity for Au(III).

Table 3. Comparison of adsorption capacity of amino acid adsorbents with other available adsorbents.

Adsorbents	pH	T (°C)	Qm (mg/g)	Ref.
2-AMPR	2.4 ± 0.2	-	537.613	[24]
DACS-TA	2.0	35	298.5	[40]
Zr-MOF	2.0	-	374.866	[41]
Ni _{0.6} Fe _{2.4} O ₄ nanoparticles	4.0	25	383.9	[42]
APS-LCP	4.0	30	261.36	[25]
ArgR	2.0	30	396.8	This work
HisR	2.0	30	636.9	This work
MetR	2.0	30	549.5	This work
CysR	2.0	30	769.2	This work

3.2.4. Thermodynamics: Effect of Temperature on Adsorption

The main thermodynamic parameters in free energy (ΔG), enthalpy (ΔH), and entropy (ΔS) for the Au(III) ion adsorption were determined at 298–318 K. The thermodynamic parameters were determined using the Van’t Hoff equation (Equations (9) to (10)) and are listed in Table 4 [43].

$$\ln K_d = \frac{\Delta S}{R} - \frac{\Delta H}{RT} \tag{9}$$

$$\Delta G = \Delta H - T\Delta S \tag{10}$$

where K_d is the equilibrium constant obtained from Q_e/C_e , R is the universal gas constant (8.3144 J/mol × K), and T is the temperature (K).

Table 4. Thermodynamic parameters of the adsorption of Au(III) ions on amino acid resins.

Adsorbents	ΔH (KJ/mol)	ΔS (J/mol/K)	ΔG (KJ/mol)				R^2
			298 K	303 K	308 K	318 K	
ArgR	8.5453	52.2784	−7.0337	−7.2981	−7.5564	−8.0792	0.9460
HisR	10.1997	60.8359	−7.9293	−8.2336	−8.5378	−9.1461	0.9695
MetR	18.8498	88.7484	−7.6270	−8.0410	−8.4847	−9.3722	0.9827
CysR	15.9659	82.5559	−8.6358	−9.0485	−9.4613	−10.2869	0.9619

Figure 5 showed Van’t Hoff plots of amino acid resins for Au(III) ion adsorption. The positive value of ΔS demonstrated that the adsorption process of Au(III) ions is a random adsorption process at the solid–liquid interface. $\Delta G < 0$, $\Delta H > 0$ means that the series of adsorption processes are endothermic and indicates a spontaneous reaction [44].

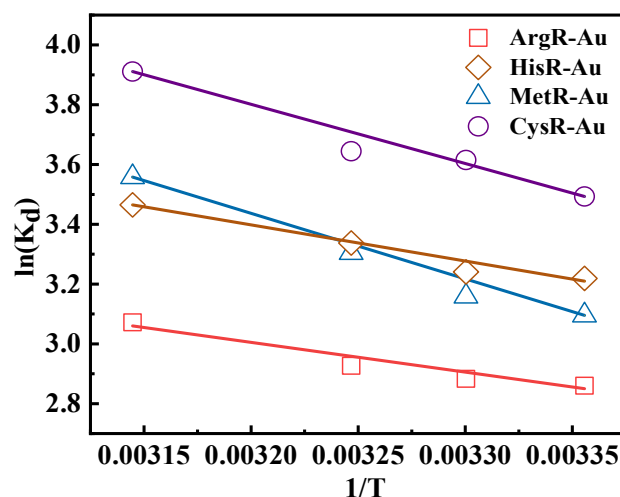


Figure 5. Van’t Hoff plots of amino acid resins for Au(III) ion adsorption (C0 = 100 mg/L, adsorbent mass = 10 mg, volume = 10 mL, pH = 2, contact time = 24 h).

3.2.5. Effect of NaCl

Aqueous metallurgy is a common method of recovering Au ions. After treatment with hydrochloric acid, a large number of Cl⁻ molecules remain. Therefore, the effect of ionic strength on the adsorption performance of an adsorbent must be investigated.

The effect of NaCl concentration on the Au(III) ion adsorption capacity of amino acid resins is shown in Figure 6a. The results show that the Au(III) adsorption efficiency of amino acid resins decreased with an increase in NaCl concentration. This is mainly because of the shielding effect of chloride ions on the electrostatic interaction between Au(III) ions and the amino acid adsorbents. This proves that the mechanism by which partial Au(III) ions were adsorbed was ion exchange. The adsorption of ArgR-Au and HisR-Au on Au(III) ions was more affected by salt concentration, but when $C_{(Au)}: C_{(NaCl)}$ was 1:1000, their adsorption efficiency was more than 80%, and the adsorption effect was also better. For MetR and CysR, although $C_{(Au)}: C_{(NaCl)}$ reached 1:2000, their Au(III) ion adsorption efficiency was still more than 85%, indicating that MetR and CysR can effectively adsorb Au(III) ions under high ionic strength. This phenomenon is consistent with the results shown in Figure 2, where it can be seen that the adsorption capacities of MetR and CysR were higher than those of ArgR-Au and HisR at pH 1.

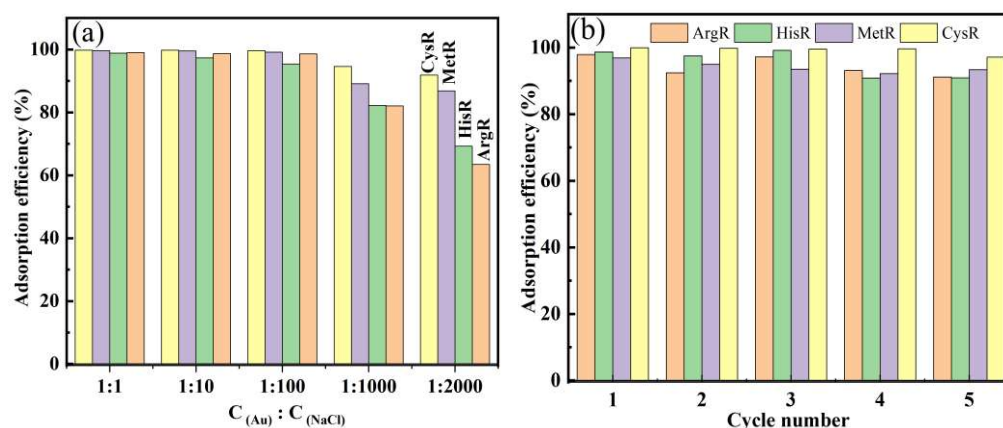


Figure 6. Effect of NaCl on Au(III) ion adsorption by amino acid resins (a) and adsorption–desorption process (b) (adsorbent mass = 10 mg, pH = 2, V = 10 mL, T = 30 °C, contact time = 24 h).

3.2.6. Reuse Property

The reuse property of the adsorbents was also investigated. A total of 1 M thiourea and 1 M HCl mixing solution were used to regenerate the amino acid adsorbents for 24 h. Figure 6b shows the adsorption efficiency after five cycles of the adsorption–desorption process. The adsorption efficiencies of the amino acid adsorbents after five cycles were almost unchanged and greater than 98%. This indicates that the amino acid adsorbents have excellent reusability and practical application prospects.

3.3. Adsorption Mechanism

3.3.1. XRD

The XRD analysis of amino acid resins before and after Au(III) ion adsorption is shown in Figure 7. The formation of Au(0) after adsorption was further confirmed by the XRD spectrum; the new peaks at 38.13°, 44.38°, 64.64°, 77.59°, and 82.11° corresponded to five diffraction peaks at the (111), (200), (220), (311), and (222) crystal faces of Au(0), which appeared after adsorption, suggesting the Au(III) ion recovery was carried out via an adsorption–reduction mechanism [3,24].

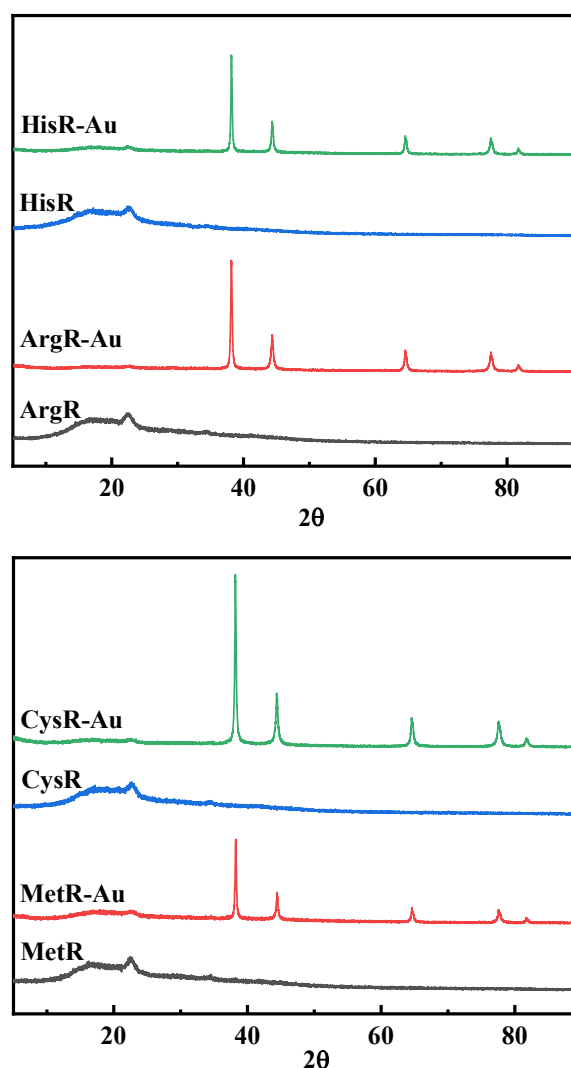


Figure 7. XRD spectra of Au-loaded amino acid resins.

3.3.2. XPS Analysis

Figure 8 illustrates the XPS spectra of amino acid resins before and after adsorption. The wide-scan spectra are shown in Figure 8a. The dominant peaks of ArgR and HisR were C1s, O1s, and N1s, and the dominant peaks of MetR and CysR were C1s, O1s, N1s, and S2p, indicating that the four amino acids were successfully introduced into cellulose. The Au4f peak at 82–92 eV appearing after adsorption represents the adsorption of Au (III) by amino acid resins [3].

Figure 8b shows the Au high-resolution XPS spectra. Both the Au4f7/2 and Au 4f5/2 peaks could be fitted to three peaks. After adsorption, the Au (0) and Au (I) signal appeared, demonstrating that Au(III) ions were reduced to Au (I) and Au (0). This result agrees with the XRD findings [45]. Combined with the XPS and XRD results, this shows that the mechanisms by which Au was adsorbed on amino acid resins were adsorption–reduction and chelation.

3.3.3. FTIR and EDX

EDX images and FT-IR spectroscopy before and after Au(III) adsorption are shown in Figures S4–S8. It can be seen from FT-IR spectroscopy that the peak positions (C-N and C-S) shifted after gold adsorption, indicating that groups containing N and S of amino acid resins interacted with Au(III). Meanwhile, the EDX images show that a lot of Au(III) was adsorbed on the surface of the resins.

On the basis of the above analysis, the mechanism by which Au(III) was absorbed on the amino acid resins is proposed in Scheme 2. The functional atoms on the surface of the adsorbent interacted with Au(III) by ion exchange, chelation, and oxidation–reduction reactions.

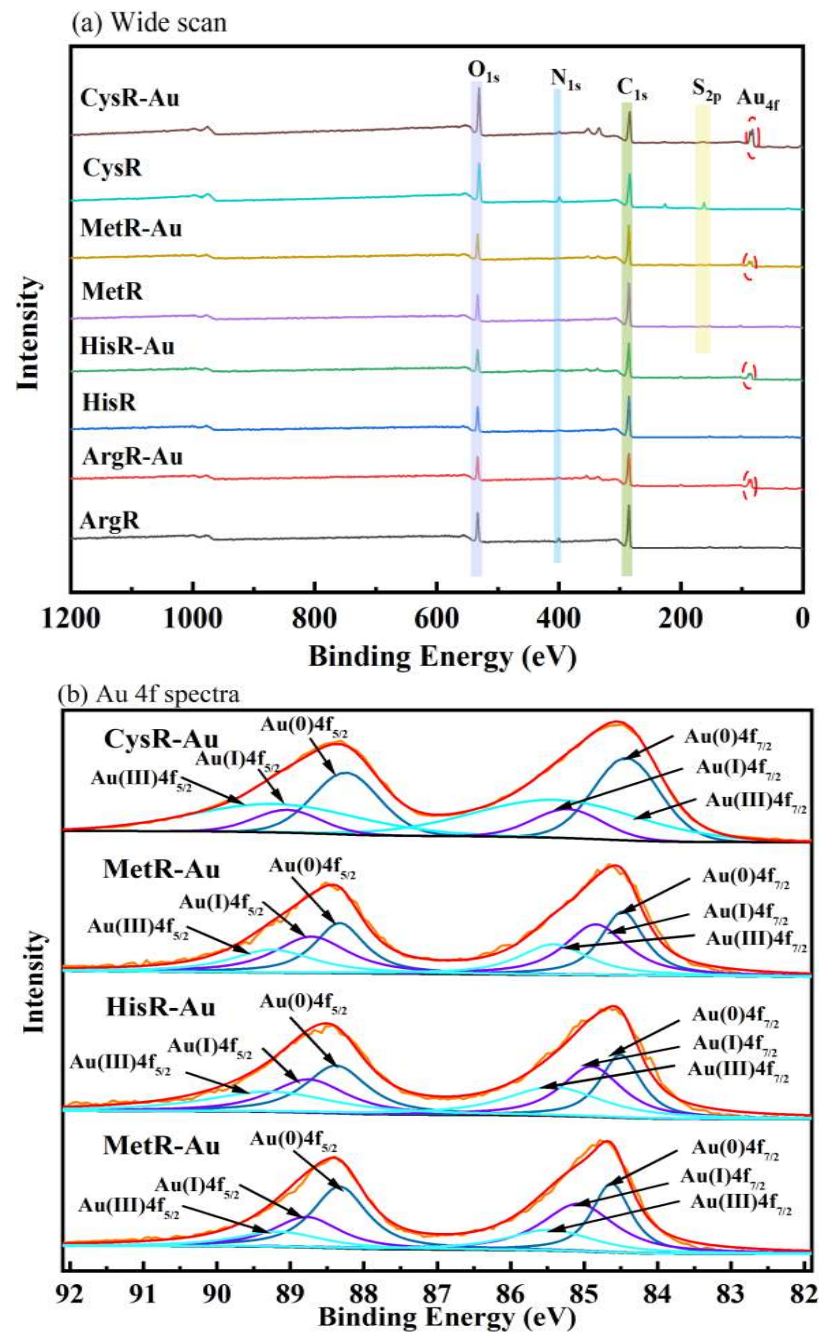
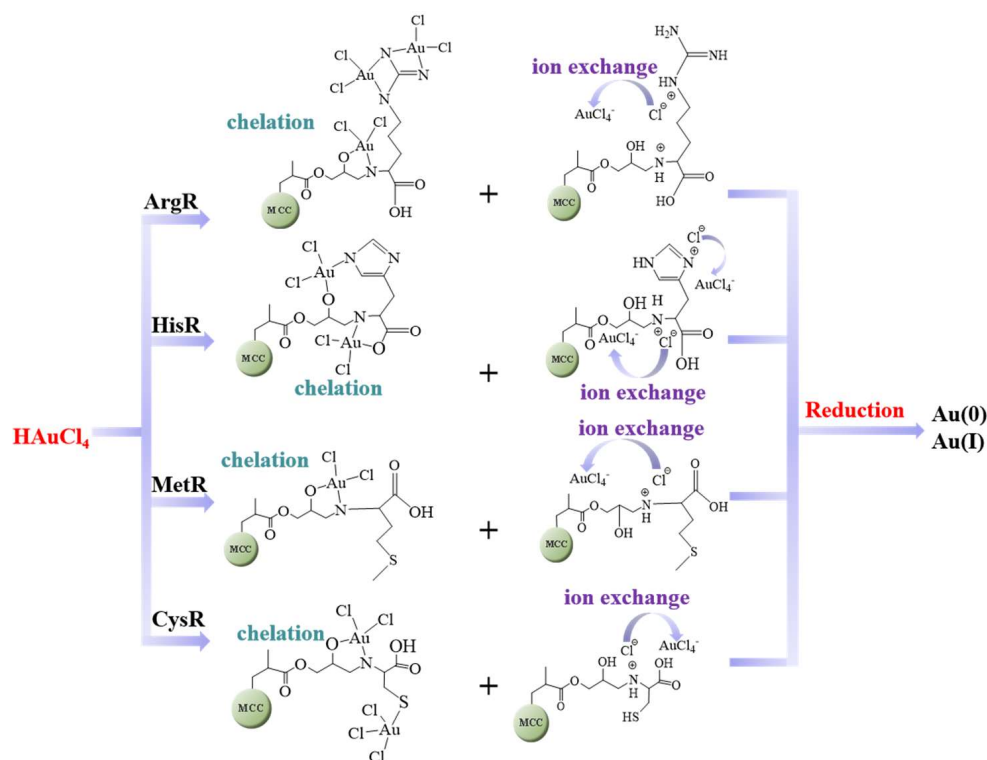


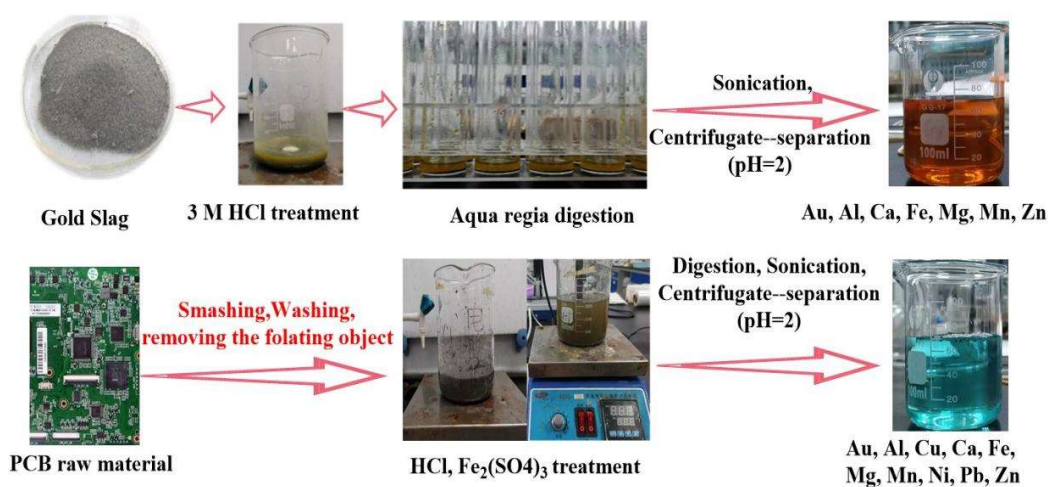
Figure 8. XPS spectra of the amino acid adsorbents before and after adsorption: wide-scan (a) and Au4f spectra (b).



Scheme 2. Mechanism of Au(III) ion adsorption onto the amino acid resins.

3.4. Practical Application of Au(III) Ion Recovery from Leaching Solutions

The recovery of gold from the leaching solution of PCB and gold slag waste is considered a potential gold resource. However, these acidic solutions also contain other base metals, such as Cu, Ni, Fe, and Zn. [10,46,47]. Therefore, it is very important that the selective recovery of trace Au(III) ions ($\mu\text{g/L}$) from practical leaching solution be investigated. In the current work, the practical application of amino acid adsorbents for Au(III) ion recovery from two practical leaching solutions, gold slag and PCB, was conducted. The leaching solution of gold slag and PCBs was prepared via the acid treatment procedure shown in Scheme 3.



Scheme 3. The leaching process of slag and PCB.

3.4.1. Gold Recovery from Gold Slag Leaching Solutions

The gold slag was obtained from the tailings of a pure quartz gold ore in Xinjiang, China. In the leaching process, gold slag with a mass of 20 g was used as a raw material, into which 3 M HCl solution was slowly added. After filtering, the solid residue obtained after the above treatment was digested with 80 mL of aqua regia (12 M HCl: 14 M HNO₃ = 3:1) for 11 cycles. Then, the solid residues were transferred into a beaker containing de-ionized water, sonicated, separated via centrifugation, and filtered. Thus, the slag leaching solution was obtained.

For the adsorption experiment, 0.02 g of amino acid resins was soaked in 5 mL of gold slag leaching solution (pH 2). The composition of the gold slag leaching solution before and after adsorption is listed in Table 5. The other metals present were Au, Al, Ca, Fe, Mg, Mn, and Zn. Figure 8a shows the adsorption efficiency of amino acid adsorbents for Au(III) ions in the presence of other metal ions. The Au(III) ion recovery efficiencies of ArgR, HisR, MetR, and CysR were 68.1%, 75.1%, 82.1%, and 74.1%, respectively.

Table 5. The composition of leaching solution before and after ArgR, HisR, MetR, and CysR adsorption.

Element	Feed (mg/L)	PCB				Raffinate (mg/L)				
		ArgR	HisR	MetR	CysR	Feed (mg/L)	ArgR	Au Slag HisR	MetR	CysR
Au	0.449	0.149	0.112	0.135	0.074	0.386	0.123	0.096	0.069	0.1
Al	108.6	108.4	108.5	108.5	107.6	351.9	345.4	347.2	345.6	336.9
Ca	252.8	245.2	246.5	246.1	245.4	261.9	264.2	262.9	264.0	261.5
Co	0.229	0.223	0.225	0.226	0.229	—	—	—	—	—
Cu	3669	3506	3559	3603	3555	—	—	—	—	—
Fe	0.37	0.36	0.36	0.38	0.38	114.7	111.1	113.1	109.5	109.7
Mg	7.530	7.403	7.379	7.385	7.376	158.6	158.6	160.6	160.2	158.1
Mn	0.530	0.509	0.512	0.505	0.506	13.89	13.83	13.76	13.73	13.64
Ni	25.38	24.68	24.68	24.51	25.36	—	—	—	—	—
Pb	35.86	34.27	34.24	34.33	34.34	—	—	—	—	—
Zn	367.8	364.3	367.1	368.8	364.5	1.232	1.352	1.081	1.299	1.218

3.4.2. Gold Recovery from PCB Leaching Solutions

For the printed circuit boards (PCBs), 20 g of PCB was used as a raw material. First, a PCB was smashed, and the objects floating in the water were removed. Then, the PCB was mixed with 3 M HCl for 3 h and 3% FeSO₄ for 8 h. The solid residues were treated with a similar process to that used for the slag residues to obtain the PCB leaching solution. The main metals present were Au, Al, Cu, Ca, Fe, Mg, Mn, Ni, Pb, and Zn. Subsequently, 0.02 g of amino acid resin was soaked in 5 mL of PCB leaching solution (pH 2). Figure 9 show the adsorption efficiency of different amino acid adsorbents for Au(III) ions in the presence of other metal ions. The Au(III) ion recovery efficiencies of ArgR, HisR, MetR, and CysR were 66.8%, 75.1%, 69.9%, and 83.5%, respectively.

Despite the existence of excessive co-leached metal ions, amino acid resins also showed a remarkable selectivity for Au(III) ions. This is mainly attributed to the presence of Au(III) ions as an anion ([AuCl₄][−] and [AuCl₃(OH)][−]) at pH 1–6. In contrast, the other competitive common metal ions existed as cations, which exhibited electrostatic repulsion to the positively charged amino acid resins. In addition, Au is a soft metal that has a higher affinity for donor atoms such as N and S atoms on amino acid resins. In conclusion, the amino acid adsorbents rarely captured any common metals except for Au(III) ions, indicating that the amino acid adsorbents possess potential for use in gold resource recovery from PCBs and gold slag.

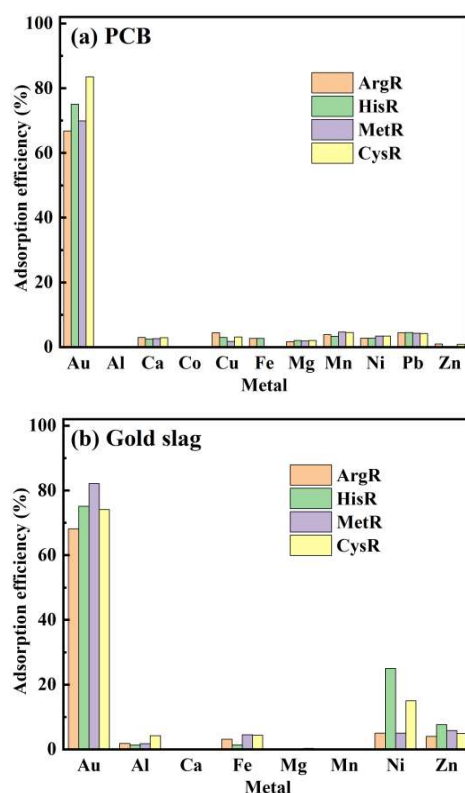


Figure 9. The adsorption efficiency of amino acid resins for different metals.

4. Conclusions

Four types of amino-acid-functionalized cellulose adsorbents for Au recovery were successfully prepared by EB radiation grafting and further modification. The amino acid resins could absorb Au(III) ions at a wide pH range. The adsorption isotherms were well fitted by the Langmuir model, and the maximum adsorption capacities of the four amino acid resins for Au(III) were 396.83 mg/g, 769.23 mg/g, 549.45 mg/g, and 636.94 mg/g. The adsorption mechanisms investigated by XRD and XPS analyses were adsorption–reduction and chelation by N and S atoms. The adsorption–desorption experiments showed that amino acid resins can be efficiently regenerated by 1 M thiourea and 1 M HCl for further Au(III) ion adsorption. The application of amino acid resins in practical leaching solutions showed that amino acid resins can effectively and selectively recover Au from practical PCB and gold slag leaching solutions.

Supplementary Materials: The following supporting information can be downloaded at: <https://www.mdpi.com/article/10.3390/polym15020321/s1>, Figure S1: SEM images of MCC, MCC-g-GMA and the amino acid resins; Figure S2: Effect of pH on Au (III) adsorption by MCC and MCC-g-GMA; Figure S3: The adsorption kinetics of amino acid resins for Au(III) ions; Figure S4: FTIR spectra of ArgR, HisR, MetR and CysR; Figure S5: EDX images of ArgR after Au (III) adsorption; Figure S6: EDX images of HisR after Au (III) adsorption; Figure S7: EDX images of MetR after Au (III) adsorption; Figure S8: EDX images of CysR after Au (III) adsorption; Table S1: BET surface areas of MCC, MCC-g-GMA and the amino acid resins; Table S2: Kinetic parameters and correlation coefficients (R^2) of the amino acid resins.

Author Contributions: Conceptualization, F.H. and J.D. and L.Z.; Investigation, J.D. and L.P.; Data curation, M.Z. and Z.D.; Writing—original draft, F.H. and J.D.; Writing—review and editing, Y.S. and L.Z. All authors have read and agreed to the published version of the manuscript.

Funding: This research received no external funding.

Institutional Review Board Statement: Not applicable.

Data Availability Statement: Not applicable.

Acknowledgments: The authors are thankful to the Analysis and Testing Center of Huazhong University of Science and Technology for its technical support. The authors would also like to thank the radiation chemistry and functional materials research group of Huazhong University of Science and Technology for the EB radiation support.

Conflicts of Interest: The authors declare no conflict of interest.

References

1. Syed, S. Recovery of Au from secondary sources—A review. *Hydrometallurgy* **2012**, *115–116*, 30–51. [[CrossRef](#)]
2. Zhang, M.; Dong, Z.; Hao, F.; Xie, K.; Qi, W.; Zhai, M.; Zhao, L. Ultrahigh and selective adsorption of Au (III) by rich sulfur and nitrogen-bearing cellulose microspheres and their applications in Au recovery from Au slag leaching solution. *Sep. Purif. Technol.* **2021**, *274*, 119016. [[CrossRef](#)]
3. Nguyen, T.S.; Hong, Y.; Dogan, N.A.; Yavuz, C.T. Au Recovery from E-Waste by Porous Porphyrin–Phenazine Network Polymers. *Chem. Mater.* **2020**, *32*, 5343–5349. [[CrossRef](#)]
4. Liu, Z.; Kou, J.; Xing, Y.; Sun, C. Recovery of Au from Ore with Potassium Ferrocyanide Solution under UV Light. *Minerals* **2021**, *11*, 387. [[CrossRef](#)]
5. Natarajan, G.; Ting, Y.P. Au biorecovery from e-waste: An improved strategy through spent medium leaching with pH modification. *Chemosphere* **2015**, *136*, 232–238. [[CrossRef](#)]
6. Dong, Z.; Zhao, L. Surface modification of cellulose microsphere with imidazolium-based ionic liquid as adsorbent: Effect of anion variation on adsorption ability towards Au(III) ions. *Cellulose* **2018**, *25*, 2205–2216. [[CrossRef](#)]
7. Yang, F.; Yan, Z.; Zhao, J.; Miao, S.; Wang, D.; Yang, P. Rapid capture of trace precious metals by amyloid-like protein membrane with high adsorption capacity and selectivity. *J. Mater. Chem. A* **2020**, *8*, 3438. [[CrossRef](#)]
8. Nguyen, N.V.; Jeong, J.; Shin, D. Simultaneous Recovery of Au and Iodine from the Waste Rinse Water of the Semiconductor Industry Using Activated Carbon. *Mater. Trans.* **2012**, *53*, 760–765. [[CrossRef](#)]
9. Pang, S.K.; Yung, K.C. Prerequisites for achieving Au adsorption by multiwalled carbon nanotubes in Au recovery. *Chem. Eng. Sci.* **2014**, *107*, 58–65. [[CrossRef](#)]
10. Zhang, L.; Zheng, Q.Q.; Xiao, S.J.; Chen, J.Q.; Jiang, W.; Cui, W.R.; Yang, G.P.; Liang, R.P.; Qiu, J.D. Covalent Organic Frameworks Constructed by Flexible Alkyl Amines for Efficient Au Recovery from Leaching Solution of E-Waste. *Chem. Eng. J.* **2021**, *426*, 131865. [[CrossRef](#)]
11. Mon, M.; Ferrando-Soria, J.; Grancha, T.; Fortea-Pérez, F.R.; Gascon, J.; Leyva-Perez, A.; Armentano, D.; Pardo, E. Selective Au Recovery and Catalysis in a Highly Flexible Methionine-Decorated Metal-Organic Framework. *J. Am. Chem. Soc.* **2016**, *138*, 7864–7867. [[CrossRef](#)]
12. Trieu, Q.A.; Pellet-Rostaing, S.; Arrachart, G.; Traore, Y.; Kimbel, S.; Daniele, S. Interfacial study of surface-modified ZrO₂ nanoparticles with thioctic acid for the selective recovery of palladium and Au from electronic industrial wastewater. *Sep. Purif. Technol.* **2020**, *237*, 116353. [[CrossRef](#)]
13. Panzarasa, G.; Osypova, A.; Consolati, G.; Quasso, F.; Soliveri, S.; Ribera, J.; Schwarze, F.W.M.R. Preparation of a Sepia Melanin and Poly(ethylene-alt-maleic Anhydride) Hybrid Material as an Adsorbent for Water Purification. *Nanomaterials* **2018**, *8*, 54. [[CrossRef](#)]
14. Gaeta, M.; Barcellona, M.; Purrello, R.; Fragala, M.E.; D’Urso, A. Hybrid Porphyrin/DOPA-melanin film as self-assembled material and smart device for dye-pollutant removal in water. *Chem. Eng. J.* **2022**, *433*, 133262. [[CrossRef](#)]
15. Yan, J.; Huang, Y.; Miao, Y.E.; Tjiu, W.W.; Liu, T. Polydopamine-coated electrospun poly(vinyl alcohol)/poly(acrylic acid) membranes as efficient dye adsorbent with good recyclability. *Chem. Eng. J.* **2015**, *259*, 53–61. [[CrossRef](#)]
16. Pangen, B.; Paudyal, H.; Inoue, K.; Kawakita, H.; Alam, S. Selective recovery of Au(III) using cotton cellulose treated with concentrated sulfuric acid. *Cellulose* **2012**, *19*, 381–391. [[CrossRef](#)]
17. Bediako, J.K.; Choi, J.W.; Song, M.H.; Zhao, Y.; Yun, Y.S. Recovery of Au via adsorption-incineration techniques using banana peel and its derivatives: Selectivity and mechanisms. *Waste Manag.* **2020**, *113*, 225–235. [[CrossRef](#)]
18. Zhao, M.; Huang, Z.; Wang, S.; Zhang, L. Ultrahigh efficient and selective adsorption of Au(III) from water by novel Chitosan-coated MoS₂ biosorbents: Performance and mechanisms. *Chem. Eng. J.* **2020**, *401*, 126006. [[CrossRef](#)]
19. Guo, J.; Fan, X.; Li, Y.; Yu, S.; Ren, X. Mechanism of Selective Au Adsorption on Ion-Imprinted Chitosan Resin Modified by Thiourea. *J. Hazard. Mater.* **2021**, *415*, 125617. [[CrossRef](#)]
20. Dwivedi, A.D.; Dubey, S.P.; Hokkanen, S.; Fallah, R.N.; Sillanp, M. Recovery of Au from aqueous solutions by taurine modified cellulose: An adsorptive–reduction pathway. *Chem. Eng. J.* **2014**, *255*, 97–106. [[CrossRef](#)]
21. Dong, Z.; Wang, Y.; Wen, D.; Peng, J.; Zhao, L.; Zhai, M.L. Recent progress in environmental applications of functional adsorbent prepared by radiation techniques: A review. *J. Hazard. Mater.* **2022**, *424*, 126887. [[CrossRef](#)] [[PubMed](#)]
22. Du, J.; Zhang, M.; Dong, Z.; Yang, X.; Zhao, L. Facile fabrication of tannic acid functionalized microcrystalline cellulose for selective recovery of Ga(III) and In(III) from potential leaching solution. *Sep. Purif. Technol.* **2022**, *286*, 120442. [[CrossRef](#)]
23. Fotoohi, B.; Mercier, L. Some insights into the chemistry of Au adsorption by thiol and amine functionalized mesoporous silica in simulated thiosulfate system. *Hydrometallurgy* **2015**, *156*, 28–39. [[CrossRef](#)]

24. Dong, Z.; Liu, J.; Yuan, W.; Yi, Y.; Zhao, L. Recovery of Au(III) by radiation synthesized aminomethyl pyridine functionalized adsorbents based on cellulose. *Chem. Eng. J.* **2016**, *283*, 504–513. [[CrossRef](#)]
25. Saman, N.; Rashid, M.U.; Lye, J.W.P.; Mat, H. Recovery of Au(III) from an aqueous solution by aminopropyltriethoxysilane-functionalized lignocellulosic based adsorbents. *React. Funct. Polym.* **2018**, *123*, 106–114. [[CrossRef](#)]
26. Yang, X.; Pan, Q.; Ao, Y.; Du, J.; Zhao, L. Facile preparation of L-cysteine-modified cellulose microspheres as a low-cost adsorbent for selective and efficient adsorption of Au(III) from the aqueous solution. *Environ. Sci. Pollut. Res.* **2020**, *27*, 38334–38343. [[CrossRef](#)]
27. Kotte, P.; Yun, Y.S. L-cysteine impregnated alginate capsules as a sorbent for Au recovery. *Polym. Degrad. Stabil.* **2014**, *109*, 424–429. [[CrossRef](#)]
28. Dong, Z.; Zhao, J.; Du, J.; Li, C.; Zhao, L. Radiation synthesis of spherical cellulose-based adsorbent for efficient adsorption and detoxification of Cr(VI). *Radiat. Phys. Chem.* **2016**, *126*, 68–74. [[CrossRef](#)]
29. Dong, Z.; Du, J.F.; Wang, A.; Yang, X.; Zhao, L. Removal of methyl orange and acid fuschin from aqueous solution by guanidinium functionalized cellulose prepared by radiation grafting. *Radiat. Phys. Chem.* **2022**, *198*, 110290. [[CrossRef](#)]
30. Peng, L.; Zhang, M.; Dong, Z.; Qi, W.; Zhai, M.; Zhao, L. Efficient and selective adsorption of Pd(II) by amino acid-functionalized cellulose microspheres and their applications in palladium recovery from PCBs leaching solution. *Sep. Purif. Technol.* **2022**, *301*, 122307. [[CrossRef](#)]
31. Dong, Z.; Yang, X.; Pan, Q.; Ao, Y.; Du, J.; Zhai, M.; Zhao, L. Performance and mechanism of selective adsorption of silver to L-cysteine functionalized cellulose microsphere. *Cellulose* **2020**, *27*, 3249–3261. [[CrossRef](#)]
32. Lin, G.; Wang, S.; Zhang, L.; Hu, T.; Peng, J.; Cheng, S.; Fu, L.; Srinivasakannan, C. Selective recovery of Au(III) from aqueous solutions using 2-aminothiazole functionalized corn bract as low-cost bioadsorbent. *J. Clean. Prod.* **2018**, *196*, 1007–1015. [[CrossRef](#)]
33. Du, J.; Dong, Z.; Pi, Y.; Yang, X.; Zhao, L. Fabrication of Cotton Linter-Based Adsorbents by Radiation Grafting Polymerization for Humic Acid Removal from Aqueous Solution. *Polymers* **2019**, *11*, 962. [[CrossRef](#)]
34. Mosoarca, G.; Vancea, C.; Popa, S.; Dan, M.; Boran, S. Crystal Violet Adsorption on Eco-Friendly Lignocellulosic Material Obtained from Motherwort (*Leonurus cardiaca* L.). *Biomass. Polym.* **2022**, *14*, 3825. [[CrossRef](#)]
35. Du, J.F.; Wu, Y.Z.; Dong, Z.; Zhang, M.; Yang, X.; Xiong, H.; Zhao, L. Single and competitive adsorption between Indigo Carmine and Methyl orange dyes on quaternized kapok fiber adsorbent prepared by radiation technique. *Sep. Purif. Technol.* **2022**, *292*, 121103. [[CrossRef](#)]
36. Yu, J.; Lan, J.; Wang, S.; Zhang, P.; Liu, K.; Yuan, L.; Chai, Z.; Shi, W. Robust covalent organic frameworks with tailor made chelating sites for synergistic capture of U(VI) ions from highly acidic radioactive waste. *Dalton Trans.* **2021**, *50*, 3792. [[CrossRef](#)]
37. Wang, C.; Zhao, J.; Wang, S.; Zhang, L.; Zhang, B. Efficient and Selective Adsorption of Gold Ions from Wastewater with Polyaniline Modified by TrimethylPhosphate: Adsorption Mechanism and Application. *Polymers* **2019**, *11*, 652. [[CrossRef](#)]
38. Zhang, P.; Wang, L.; Du, K.; Wang, S.; Huang, Z.; Yuan, L.; Li, Z.; Wang, H.; Zheng, L.; Chai, Z.; et al. Effective removal of U(VI) and Eu(III) by carboxyl functionalized MXene nanosheets. *J. Hazard. Mater.* **2020**, *396*, 122731. [[CrossRef](#)]
39. Du, J.F.; Dong, Z.; Yang, X.; Zhao, L. Facile fabrication of sodium styrene sulfonate-grafted ethylene-vinyl alcohol copolymer as adsorbent for ammonium removal from aqueous solution. *Environ. Sci. Pollut. Res.* **2018**, *25*, 27235–27244. [[CrossRef](#)]
40. Liu, F.; Peng, G.; Li, T.; Yu, G.; Deng, S. Au(III) adsorption and reduction to gold particles on cost-effective tannin acid immobilized dialdehyde corn starch. *Chem. Eng. J.* **2019**, *370*, 228–236. [[CrossRef](#)]
41. Wang, C.; Lin, G.; Zhao, J.; Wang, S.; Zhang, L.; Xi, Y.; Li, X.; Ying, Y. Highly selective recovery of Au(III) from wastewater by thioctic acid modified Zr-MOF: Experiment and DFT calculation. *Chem. Eng. J.* **2020**, *380*, 122511. [[CrossRef](#)]
42. Zhao, J.; Wang, C.; Wang, S.; Zhang, L.; Zhang, B. Selective recovery of Au(III) from wastewater by a recyclable magnetic Ni_{0.6}Fe_{2.4}O₄ nanoparticles with mercaptothiadiazole: Interaction models and adsorption mechanisms. *J. Clean. Prod.* **2019**, *236*, 117605. [[CrossRef](#)]
43. Mladenovic, N.; Petkovska, J.; Dimova, V.; Dimitrovsk, D.; Jordanov, I. Circular economy approach for rice husk modification: Equilibrium, kinetic, thermodynamic aspects and mechanism of Congo red adsorption. *Cellulose* **2022**, *29*, 503–525. [[CrossRef](#)]
44. Du, J.F.; Fan, D.C.; Dong, Z.; Yang, X.; Zhao, L. Fabrication of quaternized sisal fiber by electron beam radiation and its adsorption of indigo carmine from aqueous solution. *Cellulose* **2022**, *29*, 5137–5149. [[CrossRef](#)]
45. Alzate, A.; Lopez, E.; Serna, C.; Gonzalez, O. Au recovery from printed circuit boards by selective breaking of internal metallic bonds using activated persulfate solutions. *J. Clean. Prod.* **2017**, *166*, 1102–1112. [[CrossRef](#)]
46. Kubota, F.; Kono, R.; Yoshida, W.; Sharaf, M.; Kolev, S.D.; Goto, M. Recovery of gold ions from discarded mobile phone leachate by solvent extraction and polymer inclusion membrane (PIM) based separation using an amic acid extractant. *Sep. Purif. Technol.* **2019**, *214*, 156–161. [[CrossRef](#)]
47. Gui, W.; Shi, Y.; Wei, J.; Zhang, Z.; Li, P.; Xu, X.; Cui, Y.; Yang, Y. Synthesis of N-(3-aminopropyl)imidazole-based poly(ionic liquid) as an adsorbent for the selective recovery of Au(III) ions from aqueous solutions. *New J. Chem.* **2020**, *44*, 20387–20395. [[CrossRef](#)]

Disclaimer/Publisher's Note: The statements, opinions and data contained in all publications are solely those of the individual author(s) and contributor(s) and not of MDPI and/or the editor(s). MDPI and/or the editor(s) disclaim responsibility for any injury to people or property resulting from any ideas, methods, instructions or products referred to in the content.